

pubs.acs.org/JPCL Letter

## Enhanced Photoluminescence of All-Inorganic Manganese Halide Perovskite-Analogue Nanocrystals by Lead Ion Incorporation

Qian Meng, Liya Zhou, Qi Pang,\* Xingli He, Tingying Wei, and Jin Zhong Zhang\*



Cite This: J. Phys. Chem. Lett. 2021, 12, 10204-10211



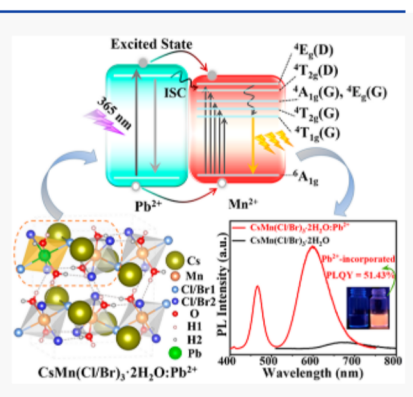
**ACCESS** 

Metrics & More

Article Recommendations

Supporting Information

**ABSTRACT:** Herein, we develop an effective approach for incorporating lead (Pb) ions into manganese (Mn) halide perovskite-analogue nanocrystals (PA NCs) of CsMn(Cl/Br)<sub>3</sub>·2H<sub>2</sub>O via room-temperature supersaturation recrystallization. Pb<sup>2+</sup>-incorporated Mn-PA NCs exhibit strong orange emission upon UV light illumination, a peak centered at 600 nm assigned to Mn<sup>2+</sup> transition ( ${}^4\Gamma_{1g} \rightarrow {}^6A_{1g}$ ) with a photoluminescence quantum yield (PLQY) of 41.8% compared to the pristine Mn-PA NCs with very weak PL (PLQY = 0.10%). The significant enhancement of PLQY is attributed to the formation of [Mn(Cl/Br)<sub>4</sub>(OH)<sub>2</sub>]<sup>4-</sup>-[Pb(Cl/Br)<sub>4</sub>(OH)<sub>2</sub>]<sup>4-</sup>-[Mn(Cl/Br)<sub>4</sub>(OH)<sub>2</sub>]<sup>4-</sup> chain network structure, in which Pb<sup>2+</sup> effectively dilutes the Mn<sup>2+</sup> concentration to reduce magnetic coupling between Mn<sup>2+</sup> pairs to relax the spin and parity selection rules. In addition, excited energy can effectively transfer from the [Pb(Cl/Br)<sub>4</sub>(OH)<sub>2</sub>]<sup>4-</sup> unit to Mn<sup>2+</sup> luminescence centers owing to the low activation energy. Pb<sup>2+</sup>-incorporated PA NCs also exhibit excellent stability. The combined strong PL and high stability make Pb<sup>2+</sup>-incorporated Mn-based PA NCs an excellent candidate for potential optronic applications.



Lead halide perovskite nanocrystals (PNCs) have fascinating photoelectric properties and strong potential for applications. However, lead toxicity and low stability are two major issues. Therefore, there is interest in developing less lead or lead-free perovskites using different metal ions to replace Pb<sup>2+</sup>. For example, Hao et al. substituted Pb<sup>2+</sup> with Sn<sup>2+</sup> and Wu et al. substituted Pb<sup>2+</sup> with Ge<sup>2+</sup>, which have similar electronic structures to Pb<sup>2+</sup>, to obtain ASnX<sub>3</sub> and AGeX<sub>3</sub> perovskites (A = organic ions or Cs; X = Cl, Br, and I). However, Sn<sup>2+</sup> and Ge<sup>2+</sup> are unstable in air and easily oxidized to Sn<sup>4+</sup> and Ge<sup>4+</sup>. Other lead-free PNCs include Sb-based Cs<sub>4</sub>CuSb<sub>2</sub>Cl<sub>12</sub>, Bi-based Cs<sub>2</sub>AgBiBr<sub>6</sub>, and In-based Cs<sub>2</sub>AgInCl<sub>6</sub> double PNC structures as well as ternary Cs<sub>3</sub>Bi<sub>2</sub>X<sub>9</sub> (X = Cl, Br). However, they tend to have low defect tolerance and show moderate photoelectric performance.

Mn<sup>2+</sup> is a commonly used dopant for altering magnetic, electrical and optical properties of materials. <sup>13–17</sup> Introduction of Mn<sup>2+</sup> into perovskite host lattice significantly increases the stability and luminescence performance of the crystal structure. <sup>18–20</sup> Due to the advantages of low toxicity and high abundance of Mn as well as the Mn<sup>2+</sup> d–d transition with emission featuring a large Stokes shift and long excited state lifetime, Mn<sup>2+</sup> has been considered as an efficient light emission center in metal halide perovskites. <sup>21</sup> Replacing Pb<sup>2+</sup> with Mn<sup>2+</sup> to obtain Mn-based perovskites, including organic—inorganic hybrid and all-inorganic manganese-based perovskites, has been studied in recent years. <sup>18,21–24</sup> For Mn-based perovskites, the absorption and emission of Mn<sup>2+</sup> are strongly dependent on its coordination environment and the distance

between the Mn<sup>2+</sup> ions.<sup>25</sup> The tetrahedral coordination Mn<sup>2+</sup> shows a green emission (500-550 nm) with narrow full width at half-maximum (fwhm) (25-60 nm) while the octagonal coordination  $Mn^{2+}$  shows an orange-red emission (>600 nm) with broad fwhm (>60 nm). Nevertheless, the d-d transition of Mn2+, determined by spin and parity selection rules, is concentration-dependent with Mn-Mn coupling at high concentrations resulting in low photoluminescence quantum yield (PLQY).<sup>28</sup> To solve this problem, incorporating with other metal ions to fabricate heterometallic perovskite to dilute Mn concentration has been explored, including (C<sub>9</sub>NH<sub>2</sub>O)<sub>9</sub>[Pb<sub>3</sub>Br<sub>11</sub>](MnBr<sub>4</sub>)<sup>29</sup> and (C<sub>5</sub>H<sub>14</sub>N<sub>2</sub>)<sub>2</sub>Pb<sub>4</sub>MnCl<sub>14</sub>.<sup>30</sup> Strong coupling between Pb and Mn induces effective energy transfer from Pb-based octahedron unit to luminescent Mn centers.31 As a result, dual emission has been observed in Pb-Mn bimetallic perovskites consisting of a Mn<sup>2+</sup>-based d-to-d transition and a Pb<sup>2+</sup>-based excitonic emission. However, the existence of labile organic components is not ideal for practical applications. Therefore, all-inorganic Mn-based heterometallic luminescent perovskites with small amount of Pb are highly desired.

Received: September 13, 2021 Accepted: October 8, 2021 Published: October 13, 2021





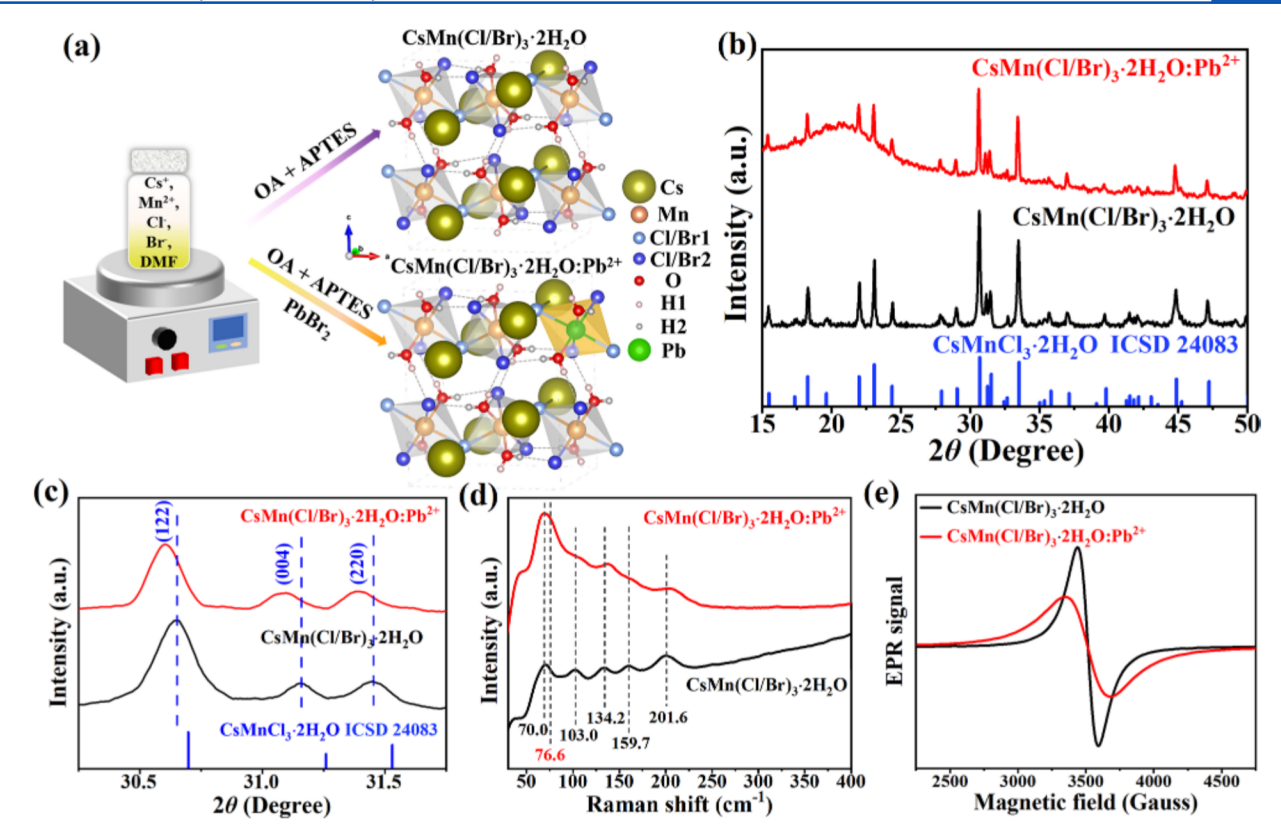


Figure 1. (a) Schematic illustration of the synthesis of Mn-based PA NCs with different precursors and the crystal structures of CsMn(Cl/Br)<sub>3</sub>·2H<sub>2</sub>O and CsMn(Cl/Br)<sub>3</sub>·2H<sub>2</sub>O:Pb<sup>2+</sup> (hydrogen bonds O-H···Cl depicted as black dashed lines). (b) XRD patterns. (c) Local enlarged view of crystal planes in XRD patterns. (d) Raman spectra. (e) X-band EPR spectra of pristine and Pb<sup>2+</sup>-incorporated CsMn(Cl/Br)<sub>3</sub>·2H<sub>2</sub>O PA NCs.

CsMnCl<sub>3</sub>·2H<sub>2</sub>O possesses a quasi-one-dimensional chain structure with  $MnX_6$  (X = Cl or OH) octahedra. Such chainlike structures will likely exhibit less concentration quenching than three-dimensional structures. Furthermore, the chain-like structure with corner-sharing MnX<sub>6</sub> octahedra can help distinguish the effects of magnetic coupling, lattice symmetry, and crystal field strength on the PL properties of Mn<sup>2+</sup>. <sup>19</sup> Herein, we report on the synthesis of Pb<sup>2+</sup>-incorporated CsMn(Cl/Br)<sub>3</sub>·2H<sub>2</sub>O perovskite-analogue nanocrystals (PA NCs) by room-temperature supersaturation recrystallization. The crystal structure of Pb<sup>2+</sup>-incorporated and pristine Mn-PA NCs was determined by X-ray diffraction (XRD) while the morphology was characterized by transmission electron microscopy (TEM). X-ray photoelectron spectroscopy (XPS) and Raman spectroscopy were used to further characterize the electronic and crystal structures. Optical studies found that Pb<sup>2+</sup>-incorporated PA NCs exhibit a strong PL band that peaked at 600 nm assigned to a 3d<sup>5</sup> Mn<sup>2+</sup> transition ( $^4T_{1g} \rightarrow$  $^6A_{1g}$ ), with a PLQY of 41.8% compared to 0.10% for the pristine Mn-PA NCs. Furthermore, Pb<sup>2+</sup>-incorporated PA NCs also show excellent stability in polar solvents attributed to a SiO<sub>2</sub> layer on the PA NCs surface formed due to hydrolysis of the 3-aminopropyltriethoxysilane (APTES) ligand used. This work demonstrates that the Pb<sup>2+</sup> incorporation can substantially improve the PL of the CsMn(Cl/Br)<sub>3</sub>·2H<sub>2</sub>O PA NCs.

Pristine and Pb<sup>2+</sup>-incorporated PA NCs were synthesized via a room temperature supersaturated recrystallizations approach as illustrated in Figure 1a. The crystal structures of pristine and Pb<sup>2+</sup>-incorporated PA NCs have space group *Pcca*, and both possess a quasi-one-dimensional chain of [Mn(Cl/

Br)<sub>4</sub>(OH)<sub>2</sub>]<sup>4-</sup> octahedrons. Upon introducing Pb<sup>2+</sup>, some Mn<sup>2+</sup> ions were substituted by Pb<sup>2+</sup> to form a [Pb(Cl/Br)<sub>4</sub>(OH)<sub>2</sub>]<sup>4-</sup> octahedron. As a result, the Pb<sup>2+</sup>-incorporated PA NCs skeleton is formed with a [Mn(Cl/Br)<sub>4</sub>(OH)<sub>2</sub>]<sup>4-</sup> [Pb(Cl/Br)<sub>4</sub>(OH)<sub>2</sub>]<sup>4-</sup> [Mn(Cl/Br)<sub>4</sub>(OH)<sub>2</sub>]<sup>4-</sup> consecutive chain structure by sharing corner X<sup>-</sup> (X = Cl, Br or OH) in Pb<sup>2+</sup>-incorporated PA NCs and the distance between [MnX<sub>6</sub>]<sup>4-</sup> [MnX<sub>6</sub>]<sup>4-</sup> becomes shorter. Figure 1a schematically illustrates the MnX<sub>6</sub> and [MnX<sub>6</sub>]<sup>4-</sup> [PbX<sub>6</sub>]<sup>4-</sup> [MnX<sub>6</sub>]<sup>4-</sup> skeleton of the pristine and incorporated PA NCs.

All peaks in the XRD patterns of pristine and Pb<sup>2+</sup>incorporated PA NCs (Mn:Pb = 1:0.25) shown in Figure 1b can be indexed to CsMnCl<sub>3</sub>·2H<sub>2</sub>O (ICSD 24083) parameters with orthorhombic phase structures. The broad band located in the range of  $2\theta = 15-25^{\circ}$  is characteristic of amorphous silica resulting from the hydrolysis of APTES. Due to the complex reaction between APTES and the Pb<sup>2+</sup> precursor, the concentration of APTES ligands on the PA NCs surface increased after adding PbBr<sub>2</sub> precursor. A higher concentration of APTES can facilitate the formation of amorphous silica, which is similar to the previous reports. 32,33 A set of characteristic peaks in the  $2\theta$  regions of  $30^{\circ}-32^{\circ}$  can be assigned to the (122), (004) and (220) crystal planes (Figure 1c).<sup>34</sup> The diffraction peaks of CsMn(Cl/Br)<sub>3</sub>·2H<sub>2</sub>O shift to a smaller angle than that of CsMnCl<sub>3</sub>·2H<sub>2</sub>O due to the larger ions radius of Br than Cl causing lattice expansion. Similarly, with a small amount of Pb2+-incorporated (Mn:Pb 1:0.17 and 1:0.25), the XRD diffraction peaks shift monotonically to a smaller angle, consistent with the lattice expansion caused by the substitution of Mn<sup>2+</sup> (97 pm) by Pb<sup>2+</sup> (133 pm). However, with more  $Pb^{2+}$  incorporated (Mn:Pb = 1:0.50), a three-dimensional (3D)  $CsPb(Cl/Br)_3:Mn^{2+}$  cubic phase is formed (Figure S1) due to lower bond energy of Pb-Cl/Br than that of Mn-X (X = Cl, Br or OH).<sup>35</sup>

In order to monitor the evolution of crystal structure before and after incorporating Pb2+, Raman spectra of the PA NCs were measured using a 532 nm laser at room temperature. As shown in Figure 1d, the sample without Pb<sup>2+</sup> shows peaks at 70.0, 103.0, 134.2, 159.7, and 201.6 cm<sup>-1</sup>. The Raman peak at 70.0 cm<sup>-1</sup> is mainly derived from the out-of-phase oscillations of ionic slabs (without the contribution of central Cl/Br atoms) and the out-of-phase oscillations of the edge located Cs atoms.<sup>31</sup> The signals at 134.2 and 201.6 cm<sup>-1</sup> are identified as the in-plane and out-plane motions of Mn and Cl/Br atoms while the combinations of in-plane vibrations of Cs and Cl/Br atoms are located at 103.0 and 159.7 cm<sup>-1</sup>.31 The results support the existence of Cs-Mn-Cl/Br. However, the Pb<sup>2+</sup>incorporated sample has an extra strong peak at 76.6 cm<sup>-1</sup> which could be due to the [PbX<sub>6</sub>]<sup>4-</sup> octahedron.<sup>36-38</sup> Meanwhile, the increased intensity of the peaks at 70.0, 134.2, and 201.6 cm<sup>-1</sup> indicates the enhancement of the outof-plane distortion in  $[MnX_6]^{4-}$  octahedron after  $Pb^{2+}$  incorporating, which breaks the symmetry of the lattice. <sup>31</sup> This result supports the successful incorporating of Pb<sup>2+</sup> and is consistent with XRD results.

The surrounding environment of Mn<sup>2+</sup> ions in the samples were studied by X-band EPR spectra. As shown in Figure 1e, all of the EPR spectra show one broad background formant from Mn<sup>2+</sup> centers and the absence of the well-defined 6-fold hyperfine splitting indicates the severe spin relaxation due to the high Mn concentration. <sup>19,39,40</sup> Moreover, the line width of the Pb<sup>2+</sup>-incorporated sample is broader than that of the pristine sample, and the EPR signal intensity of the former is weaker. In general, weaker spin—spin coupling leads to a broader and weaker EPR signal; <sup>19</sup> thus, the magnetic exchange interaction between Mn<sup>2+</sup> ions seems to be weakened by Pb<sup>2+</sup> incorporation. The EPR spectra are consistent with the magnetic hysteresis loops (Figure S2), both of which indicate weaker Mn—Mn interaction in the Pb<sup>2+</sup>-incorporated sample. <sup>19,41</sup>

Figure 2 shows TEM and HRTEM images of the pristine and  $Pb^{2+}$ -incorporated PA NCs. Both are most spherical with

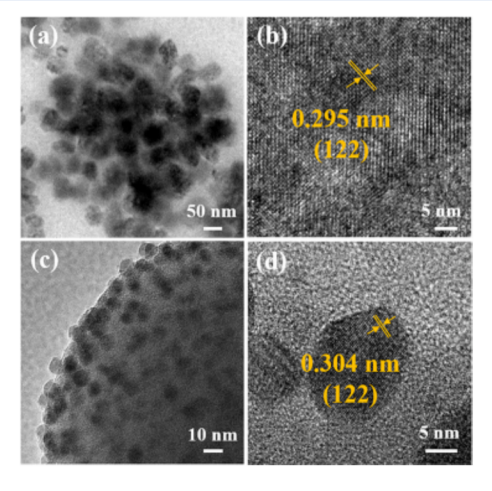


Figure 2. TEM and HRTEM images of (a, b) pristine CsMn(Cl/Br)<sub>3</sub>·2H<sub>2</sub>O PA NCs and (c, d) CsMn(Cl/Br)<sub>3</sub>·2H<sub>2</sub>O:Pb<sup>2+</sup> PA NCs.

an average diameter of  $50.0 \pm 4.4$  nm and  $7.0 \pm 1.0$  nm for the pristine and Pb2+-incorporated PA NCs, respectively. Both samples exhibit a crystal structure corresponding to the (122) plane. However, the crystal lattice constant increased slightly from 0.295 nm (pristine) to 0.304 nm (Pb<sup>2+</sup>-incorporated sample) because of the larger Pb<sup>2+</sup> ions substituting for the smaller Mn<sup>2+</sup> ions, which is consistent with the XRD result. When Mn:Pb = 1:0.50, the crystal is transformed into a cubic phase (Figure S3). The PA NCs are embedded in amorphous silica matrix due to the slow hydrolysis of APTES ligand to form a SiO<sub>2</sub> layer<sup>32,42</sup> resulting in high stability performance and the incorporated PA NCs are more monodisperse than the pristine PA NCs agglomerated with several nanoparticles. The HAADF image and corresponding element mapping of Pb2+incorporated sample demonstrate uniform distributions of Cs, Mn, Pb, Br, Cl, and Si elements (Figure S4). The presence of Pb ions is further confirmed as 11.3% of Pb<sup>2+</sup> to CsMn(Cl/ Br)<sub>3</sub>·2H<sub>2</sub>O with atomic ratio calculated by formula: {[Pb]/ ([Pb] + [Mn]) × 100 in Table S1. In addition, the concentrations of Pb in the final products were determined by ICP-OES (Table S2). For a Mn-Pb ratio of 1:0.25, the concentrations of Pb in PA NCs is 25.2%.

The chemical composition and electronic properties of Pb<sup>2+</sup>incorporated PA NCs were further studied by XPS. As shown in Figure 3a, Pb  $4d_{3/2}$ , Pb  $4d_{5/2}$ , Pb  $4f_{5/2}$ , and Pb  $4f_{7/2}$  are observed in Pb<sup>2+</sup>-incorporated PA NCs besides Cs 3d<sub>3/2</sub>, Cs 3d<sub>5/2</sub>, Mn 2p, O 1s, N 1s, C 1s, Cl 2s, Br 3s, Cl 2p, Cs 4d, and Br 3d.<sup>43</sup> As shown in Figure 3b-f, after Pb<sup>2+</sup>-incorporation, two Cs 3d peaks at 738.4 and 724.4 eV corresponding to Cs  $3d_{3/2}$  and Cs  $3d_{5/2}$  both move 0.2 eV toward lower binding energy to 738.2 and 724.2 eV, the Mn 2p<sub>1/2</sub> and Mn 2p<sub>3/2</sub> peaks shift to lower binding energy by 0.2 eV to 653.7 and 641.8 eV, the two Cl  $2p_{1/2}$  and Cl  $2p_{3/2}$  peaks have a shift of 0.2 eV toward low binding energy to 200.1 and 198.4 eV, and the two Br  $3d_{3/2}$  and Br  $3d_{5/2}$  peaks also have a shift of 0.4 eV to lower binding energy at 69.1 and 68.0 eV, respectively. Two Pb 4f peaks at 143.5 and 138.6 eV are attributed to Pb 4f<sub>5/2</sub> and Pb 4f<sub>7/2</sub>, confirming the presence of Pb-Cl/Br.<sup>44</sup> The coordination bonds formed by Cs-Cl/Br and Mn-Cl/Br are weakened, and the peaks of Cs 3d, Mn 2p, Cl 2p, and Br 3d all move toward lower binding energy with respect to the pristine sample due to Pb<sup>2+</sup> incorporating. The percentage of each element was estimated from the XPS measurements (Table

UV-vis absorptions spectra of the pristine and Pb<sup>2+</sup>incorporated samples shown in Figure 4a are similar. The band at 520 nm shows a relatively feeble absorbance corresponds to  $^6A_{1g}$  to  $^4T_{1g}$  transition due to the low spin-forbidden in Mn octahedral coordination. The spectrum of the Pb<sup>2+</sup>-incorporated sample has a onset at 500 nm with an exciton absorption peaks at 450 nm which can be contributed to the introduced  $[Pb(Cl/Br)_4(OH)_2]^{4-}$  octahedron. With more Pb2+ incorporated (Mn:Pb = 1:0.50), obvious exciton absorption peaks at 420, 365 are observed (Figure S5a). In order to better visualize the exciton transfer of Pb2+incorporated PA NCs, the PLE spectra of powder samples collected at the Mn2+ emission wavelength were measured and shown in Figure S6. For the pristine sample, all of the peaks originated from the d-d transitions in the octahedrally coordinated Mn<sup>2+</sup> ions.<sup>23</sup> In addition to the excitation from Mn<sup>2+</sup> ions, the sample with Pb<sup>2+</sup> incorporation shows an additional significant excitation peak at 365 nm that confirms the existence of octahedral coordination of Pb2+ ions. We

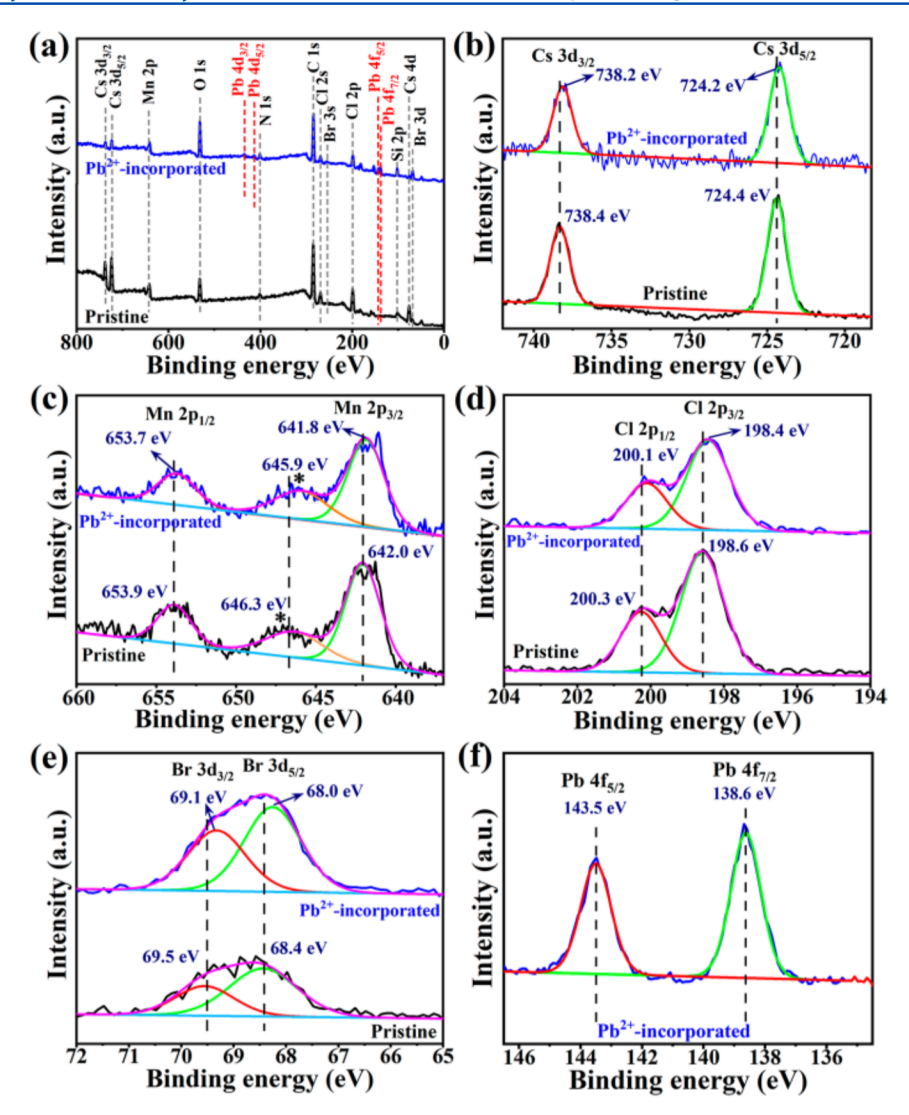


Figure 3. (a) XPS survey spectra and high-resolutions XPS spectra of (b) Cs, (c) Mn, (d) Cl, (e) Br, and (f) Pb of pristine and Pb<sup>2+</sup>-incorporated (Mn:Pb = 1:0.25) ( $\lambda_{ex}$  = 365 nm) CsMn(Cl/Br)<sub>3</sub>·2H<sub>2</sub>O PA NCs. The satellite peaks of Mn<sup>2+</sup> were marked with asterisks in part c.

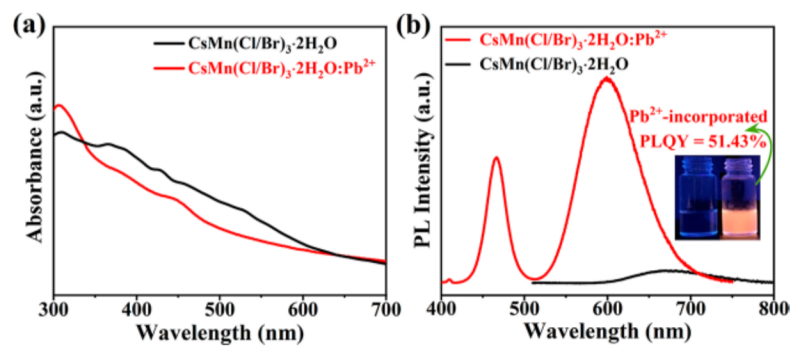


Figure 4. (a) UV-vis absorbance and (b) PL spectra of pristine ( $\lambda_{ex}$  = 420 nm) and Pb<sup>2+</sup>-incorporated CsMn(Cl/Br)<sub>3</sub>·2H<sub>2</sub>O PA NCs (Mn:Pb = 1:0.25) ( $\lambda_{ex}$  = 365 nm) (inset: a photograph of the respective samples under a 365 nm UV lamp).

further characterized the PL of the two kinds of PA NCs (Figure 4b). When excited at 420 nm, a very weak PL emission band that peaked around 670 nm (PLQY = 0.1%) was detected for the pristine PA NCs due to the spin and parity selection rules of Mn in octahedral coordination. When excited at 365 nm, the Pb $^{2+}$ -incorporated PA NCs exhibits

dual-emission, one at 465 nm with an fwhm of 27 nm and another broad band that peaked around 600 nm (fwhm  ${\sim}82$  nm). The narrow band (bluer band) is assigned to the intrinsic exciton emission of lead-halide units ([PbX<sub>6</sub>]<sup>4–</sup>), while the broader band is assigned to a 3d<sup>5</sup> intraconfigurational Mn<sup>2+</sup> transition ( $^4T_{1g} \rightarrow ^6A_{1g}$ ).